Mapping Antibiotic Resistance in Baffin Bay
Final Report

Publication CBBEP – 198
Project Number - 2529
February 2026

Prepared by:
Nora Bleth, Laboratory Manager
Kristen Waddell, Laboratory Technician
Lee Pinnell, Co-Principal Investigator
Jeffrey W. Turner, Co-Principal Investigator
Texas A&M University-Corpus Christi
6300 Ocean Drive, TH240
Corpus Christi, Texas 78412
Phone: 361-825-6206
Email: jeffrey.turner@tamucc.edu

Submitted to:
Coastal Bend Bays & Estuaries Program
1305 N. Shoreline Blvd. Suite 205
Corpus Christi, TX 78401

The views expressed herein are those of the authors and do not necessarily reflect the views of CBBEP or other organizations that may have provided funding for this project.

PREPARED IN COOPERATION WITH THE TEXAS COMMISSION ON ENVIRONMENTAL QUALITY AND U.S. ENVIRONMENTAL PROTECTION AGENCY.
This project has been funded wholly or in part by the United States Environmental Protection Agency under assistance agreement C6-48000061-0 to Texas Commission on Environmental Quality. The contents of this document do not necessarily reflect the views and policies of the Environmental Protection Agency, nor does the EPA endorse trade names or recommend the use of commercial products mentioned in this document.

Table of Contents

Abbreviations

AMR	Antimicrobial Resistance
ARG	Antimicrobial Resistance Genes
CBBEP	Coastal Bend Bays & Estuaries Program
USEPA	United States Environmental Protection Agency
FIB	Fecal indicator bacteria
MPN	Most probable number
NTC	No-template control
MLS	Macrolide-lincosamide-streptogramin
PCR	Polymerase chain reaction
TAMU-CC	Texas A&M University-Corpus Christi
TCB	Texas Coastal Bend

Summary

Antimicrobial resistance, conferred by antimicrobial resistance genes (ARGs), renders critical antimicrobials and antibiotics ineffective against resistant microorganisms. Due to the global health implications, ARGs are increasingly being considered a form of pollution within the natural environment. Current research has examined resistomes in river and urbanized coastal ecosystems, leaving a gap in understanding for rural, hypersaline systems and watersheds dominated by agricultural land use. This project characterized the resistome of Baffin Bay, TX, using shotgun metagenomics on 144 water samples and assessing the geographic distribution, environmental drivers, and identity of antimicrobial resistance genes (ARGs). Baffin Bay, a hypersaline bay within a rural watershed, is well known as “the jewel of the Texas coast” for recreational water activities. In recent decades, the bay has undergone rapid declines in water quality, including brown tides, hypoxia, and fish kills. The results showed that San Fernando Creek had significantly higher ARG abundances and diversity compared to the bay and its two additional tributaries (Los Olmos and San Fernando Creeks). Seasonality had minimal impact on ARG diversity. Fecal pollution originating from cows, pigs, and humans was strongly correlated with ARG diversity, while traditional fecal indicator bacteria (FIB) were not. Aminoglycoside resistance and macrolide-lincosamide-streptogramin (MLS) resistance maintained the highest relative abundances throughout the watershed. The dominant ARG classes confer resistance to antibiotics primarily used to treat livestock. Furthermore, our results suggest that land use is a primary determinant of resistome composition and diversity.

Acknowledgements

Funding for this study was provided by the Coastal Bend Bays and Estuaries Program (CBBEP) (Contract No. 2529). Funding for the collection of samples used in this study was provided by the United States Environmental Protection Agency (USEPA) (Contract No. 02D18222). We thank the lab members of the ‘micro-omics’ team, particularly Dr. Nicole Powers, for her mentorship and assistance during the QAPP writing phase of the study.

Introduction

The spread of antimicrobial resistance (AMR) is a global health crisis that renders critical antimicrobials ineffective against resistant infections (CDC, 2019). In 2021, AMR was linked to 4.71M deaths, and the global burden is projected to exceed 39M deaths between 2025 and 2050 (Naghavi et al., 2024). Additionally, a World Bank report estimated that AMR will decrease global gross domestic product by 3.8% annually by 2050 and push 28M people into poverty (Ahmed et al., 2018). AMR is an ancient defense mechanism for single-celled organisms predating the modern use of antimicrobials (D'Costa et al., 2011; Pinnell et al., 2023). However, the drivers of AMR extend beyond the ecological and medical settings, reflecting the link between humans and the natural environment. Antimicrobial resistance genes (ARGs) constitute a human health risk and are increasingly recognized as a form of environmental pollution.

Natural environments are reservoirs for the resistome, or the aggregate of all ARGs in an ecosystem (Wright, 2007). Elevated ARG abundance and diversity occur near wastewater outfalls, urbanized shorelines, and agricultural runoff (Su et al., 2024; Zheng et al., 2021). Impaired coastal ecosystems contribute to the spread of AMR by integrating fecal pollution, residual antibiotics, seafood consumption, and recreation (Zhu et al., 2017). Coastal systems are progressively viewed through the One Health lens as reservoirs that contribute to the global spread of AMR (Kim & Cha, 2021).

Most resistome studies have focused on temperate, river-dominated, or heavily urbanized estuaries (e.g., Xu et al., 2023; Zhu et al., 2017). Hypersaline systems present a distinct ecological context in which extreme physicochemical conditions may shape resistome structure and risk in ways that differ from more typical estuaries. Elevated salinity, sulfate-rich sediments, and periodic hypoxia select for specialized microbial assemblages, potentially influencing the ARG abundance and diversity (Hatosy & Martiny, 2015). Understanding how these natural and anthropogenic pressures interact is critical for understanding resistome dynamics in hypersaline lagoons.

We conducted a comprehensive resistome analysis within the hypersaline watershed of Baffin Bay, TX, using metagenomic approaches to characterize ARG abundance and diversity. Baffin Bay faces chronic anthropogenic stressors that potentially co-select for AMR, including heavy metals, nutrients, herbicides, pesticides, oil, and fecal pollution. The three freshwater inflows (San Fernando, Petronila, and Los Olmos Creeks) are listed as impaired by elevated fecal bacteria under Section 303(d) of the Clean Water Act. A recent microbial source tracking study identified cattle, waterfowl, feral pigs, and humans (respectively) as the primary sources of fecal pollution (Powers et al., 2025). Systemic pesticide pollution has been detected in Baffin Bay, with 96% of water samples containing at least 4 pesticides, including atrazine, malathion, chlorpyrifos, bifenthrin, trifluralin, simazine, dimethoate, and metholachlor (Conkle & Hormoz-Estrabad, 2018). Additionally, the Baffin Bay watershed has a history of heavy metal pollution. One study detected various metals (e.g., barium, magnesium, strontium, zinc) in sediment

(Douglas et al., 2025). Another study in the neighboring Upper Laguna Madre correlated elevated barium concentrations (155-757µg/g) with the use of barite ($BaSO_4$) in drilling mud produced by oil and gas industries (Sharma et al., 1999). These stressors are exacerbated by restricted hydrodynamic exchange due to the barrier island, elevated salinity, and episodic hypoxia (Withers et al., 2002).

This work establishes a baseline for understanding AMR in a hypersaline system, addressing a key geographic and ecological gap in resistome research. More broadly, these results contribute to efforts to refine environmental AMR assessment and inform management prioritization in Texas Coastal Bend (TCB) watersheds.

Methods

Previous MST Study Details

A microbial source-tracking study was conducted from Oct 2022-June 2024. Detailed methods and results can be found in the Final Report for the EPA Gulf of America Division Project Award 02D18222 (Powers et al., 2025). The study collected monthly water samples over 18 months (N=216 total samples, 12 study sites, Figure 1) and quantified environmental parameters, nutrient concentrations, fecal indicator bacteria, and host-associated molecular markers using droplet digital PCR. Water samples were filtered onto 0.45µm mixed-cellulose ester or polyethersulfone (Millipore, Burlington, MA) filters, transferred to sterile conical tubes, and stored at -80°C until DNA extraction.

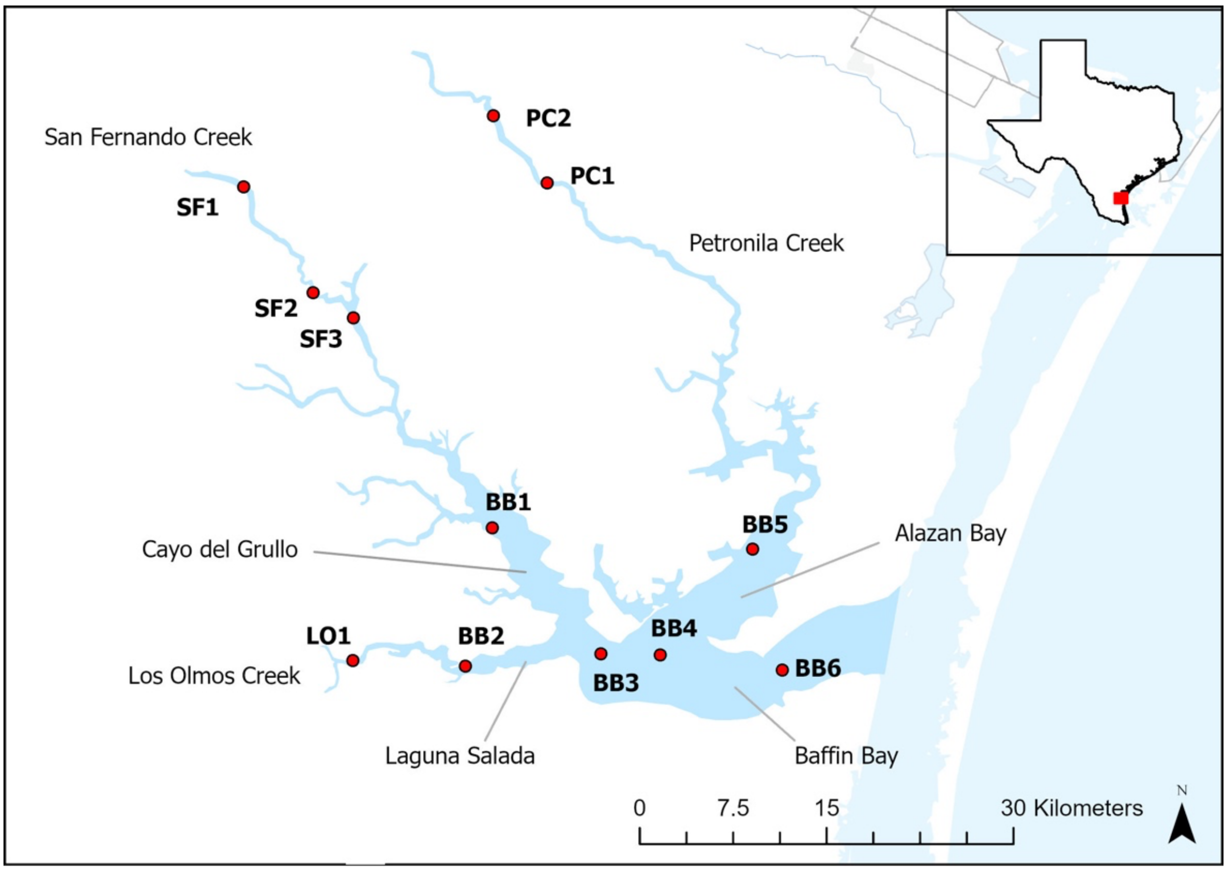

Figure 1. The red icons show the locations of the 12 sampling stations in the Baffin Bay watershed in relation to Texas and the Gulf of America. Petronila Creek (PC) and San Fernando Creek (SF) were listed as impaired prior to the start of this study (Oct 2022) and Los Olmos Creek (LO) was listed as impaired in 2024.

DNA Extraction

A subset of water samples (N=144) was chosen for shotgun metagenomic sequencing. Filters were aseptically cut into ~1cm strips, and DNA was isolated using the DNeasy PowerSoil Pro Kit (QIAGEN, Hilden, Germany) following the manufacturer's instructions (QIAGEN, 2023). The quality and quantity of the DNA were assessed using a biospectrometer (Eppendorf, Hamburg, Germany), and A_{260}/A_{280} and concentrations (µg/µL) were recorded. The DNA samples were stored at -80°C until shipped for library preparation.

Library Preparation

Sequencing libraries were prepared with the Illumina DNA Prep Kit (Illumina, San Diego, CA, USA), according to the manufacturer's instructions. The sequencing was completed at the North Texas Genome Center at the University of Texas – Arlington on an Illumina NovaSeq 6000 platform, following the manufacturer's instructions using paired-end chemistry (2x150bp). Each lane employed no-template-controls (NTC) and positive controls using Zymo Mock Community Standards to assess sequencing quality, taxonomic accuracy, and contamination.

Bioinformatics

Metagenomic analysis was conducted on the TAMU-CC high performance computing cluster (HPC). Raw reads were assessed for quality using FastQC (Andrews, 2010; Bokulich et al., 2013). Adaptors were trimmed from the sequences using trimmomatic version 0.39 (Bolger et al., 2014). The AMR++ pipeline and the MEGARes v 3.0 resistance database identified the quality and relative abundance of ARGs (Bonin et al., 2023). Details on the AMR++ pipeline and MEGARes database can be found at http://megares.meglab.org. ARGs requiring single-nucleotide polymorphism (SNP) confirmation were filtered from the dataset using the 'AmrPlusPlus_SNP' tool within the AMR++ pipeline. The count matrix produced by the AMR++ pipeline was imported into and processed with R version 4.3.1 and R Studio. Differences in resistome composition, diversity, and abundance were examined using the phyloseq, vegan, and ANCOMBC packages (Lin & Peddada, 2020; McMurdie & Holmes, 2013; Oksanen et al., 2001). Figures were generated using the ggplot, cowplot, and ggsignif packages (Ahlmann-Eltze & Patil, 2021; Almeida et al., 2019; Wilke, 2015).

Data Analysis

Changes in the resistome were examined in the context of location, season, and fecal indicator bacteria (FIB) concentration. Location was divided into four water systems: Baffin Bay (sites BB1, BB2, BB3, BB4, BB5, and BB6, N=72), Los Olmos Creek (site LO1, N=12), Petronila Creek (sites PC1 and PC2, N=24), and San Fernando Creek (sites SF1, SF2, and SF3, N=36). Samples were grouped according to collection date into spring (March, April, May), summer (June, July, August), fall (September, October, November), and winter (December, January, February). FIB was initially quantified using the Enterolert (marine samples) and Colilert-18 (freshwater samples) tests (Powers et al., 2025). The tests have a lower limit of detection (Enterolert: <10MPN/100mL, Colilert-18: <1MPN/100mL). Additionally, the USEPA and Texas Beach Watch have set risk-based thresholds for these tests (Enterolert: >104MPN/100mL and Colilert-18: >320MPN/100mL) (Texas General Land Office, n.d.; United States Environmental Protection Agency, 2011). Samples in the resistome dataset were classified as undetected, detected, or exceeded threshold based on their associated limit of detection and risk-based thresholds. If FIB data were unavailable, the sample was classified as unavailable and excluded from subsequent statistical tests.

Samples containing less than 500 ARGs were removed from downstream analyses. To assess the abundance of ARG sequences within each metagenomic sequencing library, the total number of ARGs in each sample was normalized by the total number of reads to account for differences in sequencing depth.

Alpha diversity was assessed using richness (the total number of unique observed ARGs), the Shannon-Wiener Diversity Index, and Simpson's Diversity. These metrics were calculated for system, season, and FIB level. All subsequent statistical testing used a p-value threshold of <0.05 to determine significance. A Kruskal-Wallis test, followed by a paired-end Wilcoxon test, determined whether there were significant differences in alpha diversity between systems, seasons, and FIB levels. Spearman's correlation coefficient was calculated to examine the monotonic relationships between alpha diversity and MST markers, environmental parameters, nutrient concentrations, and FIB concentrations.

ARG counts were then normalized using total sum scaling, and beta diversity was examined using Jaccard's Distance and Bray-Curtis Dissimilarity. The resulting distance matrices were ordinated, and the results were visualized using nonmetric multidimensional scaling plots. The average relative abundance of ARG classes was plotted by system. A PERMANOVA and permutation dispersion test examined beta diversity and its relationship with system and season. Differential abundance plots were generated to observe changes in individual ARG classes between systems, using Baffin Bay as a baseline and comparing it to its three tributaries.

Results

DNA Quality Control

DNA was successfully isolated from 144 water samples. Quality (A_{260}/A_{280}) ranged from 1.58 to 1.98, with a mean and median of 1.76. Concentration ranged from 14.2 to 424ng/µL, with a mean and median of 106.69 and 91.9ng/µL, respectively (Table S1). FastQC successfully trimmed adaptor sequences from reads, producing 2x151bp reads with 81.5-569.2 million reads per sample. The mean Phred score at all base positions across samples was >33.5, exceeding the minimum Q30 requirement.

ARG Abundance

The total number of normalized ARG hits varied significantly due to system ($p<2.2e^{-16}$), with San Fernando Creek containing the highest number of hits, followed by Petronila Creek, Los Olmos Creek, and Baffin Bay (Figure 2).

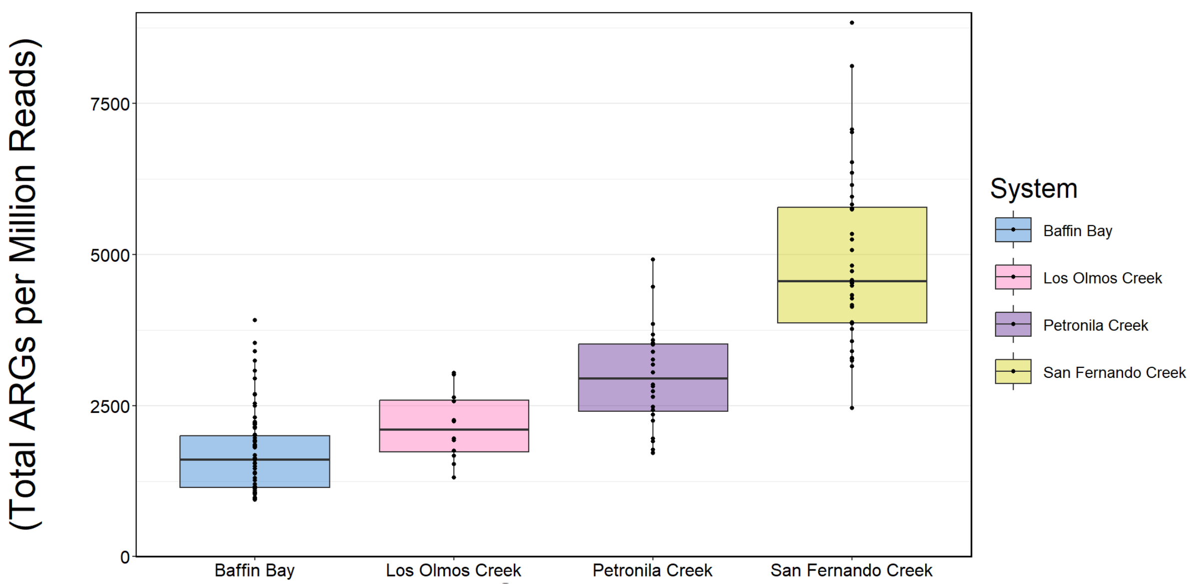

Figure 2. A boxplot of the total number of ARG hits per million reads grouped by each system. The total abundance of ARGs varied significantly across systems ($p<2.2e^{-16}$). All systems were significantly different from each other.

Alpha Diversity

Alpha diversity in Baffin Bay varied significantly by location and season. ARG richness varied significantly across all systems, with San Fernando having the highest richness, followed by Petronila Creek, Baffin Bay, and Los Olmos Creek ($p<2.2e^{-16}$). The Shannon-Wiener Diversity Index reflects the richness and evenness of ARG species, while the Simpson Diversity Index emphasizes the dominance of the most abundant ARGs. San Fernando Creek had significantly higher diversity, as measured by both the Shannon-Wiener and Simpson indices, than all other water systems ($p<1.2e^{-13}$, $p<2.4e^{-12}$). There were no significant differences in Shannon-Weiner Diversity or Simpson's Diversity within the remaining systems. Seasonality also showed significant variations in alpha diversity. While there was no significant difference in richness due to season, both Shannon-Wiener's and Simpson's diversity indexes were significantly higher during the spring season than the winter season ($p<0.05$).

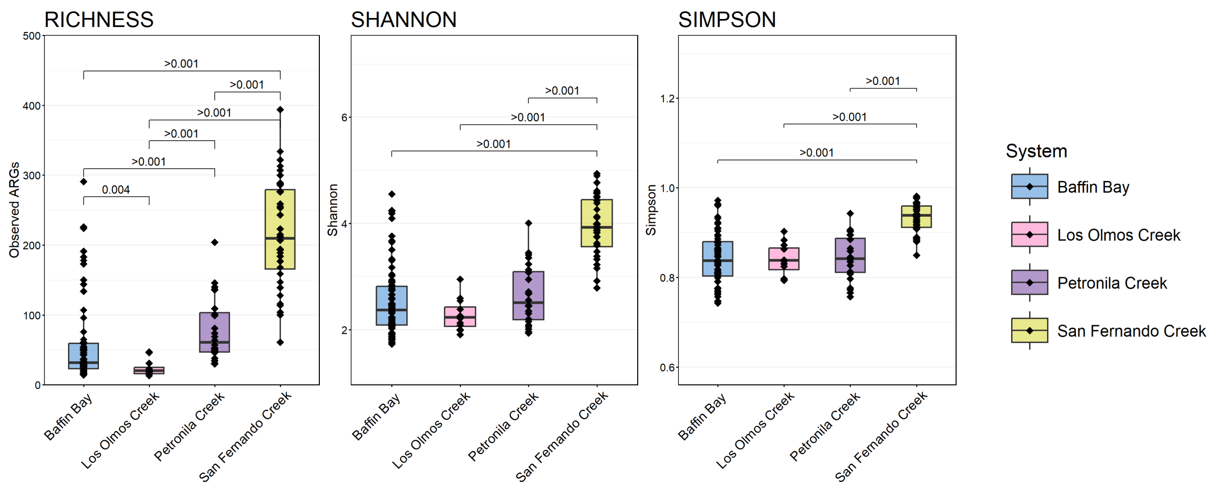

Figure 3. Each panel contains boxplots of alpha-diversity metrics (richness, Shannon-Weiner Index, Simpson's Diversity Index) calculated within each system. Significant differences between the systems are indicated by the lines grouping the two boxplots, and the associated p-values are listed above.

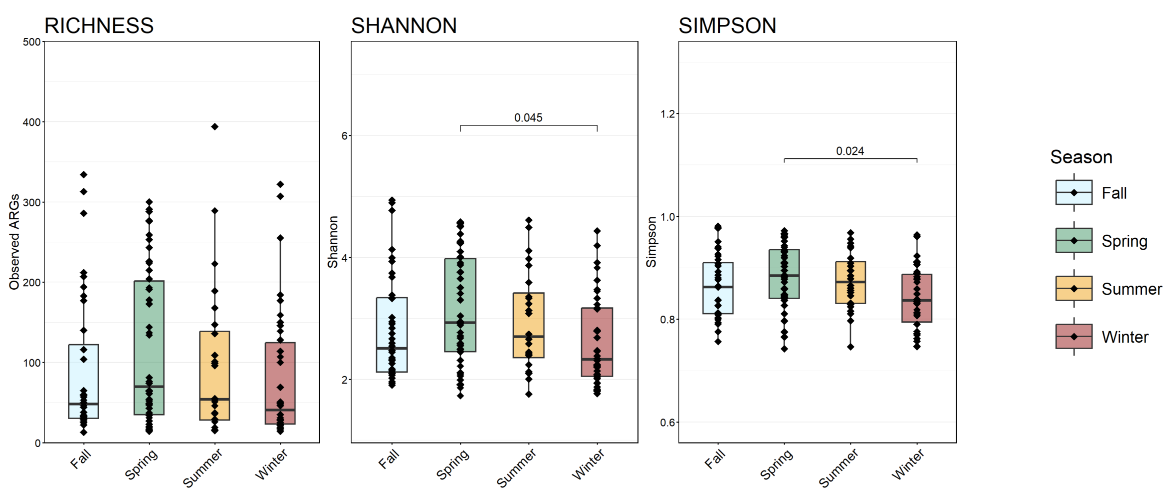

Figure 4. Each panel contains boxplots of alpha diversity metrics (richness, Shannon-Weiner Index, Simpson's Diversity Index) calculated for each season. Significant differences between the systems are indicated by the lines grouping the two boxplots, and the associated p-values are listed above.

FIB levels had no influence on alpha diversity. Additionally, there were no significant correlations between alpha diversity metrics and FIB concentrations.

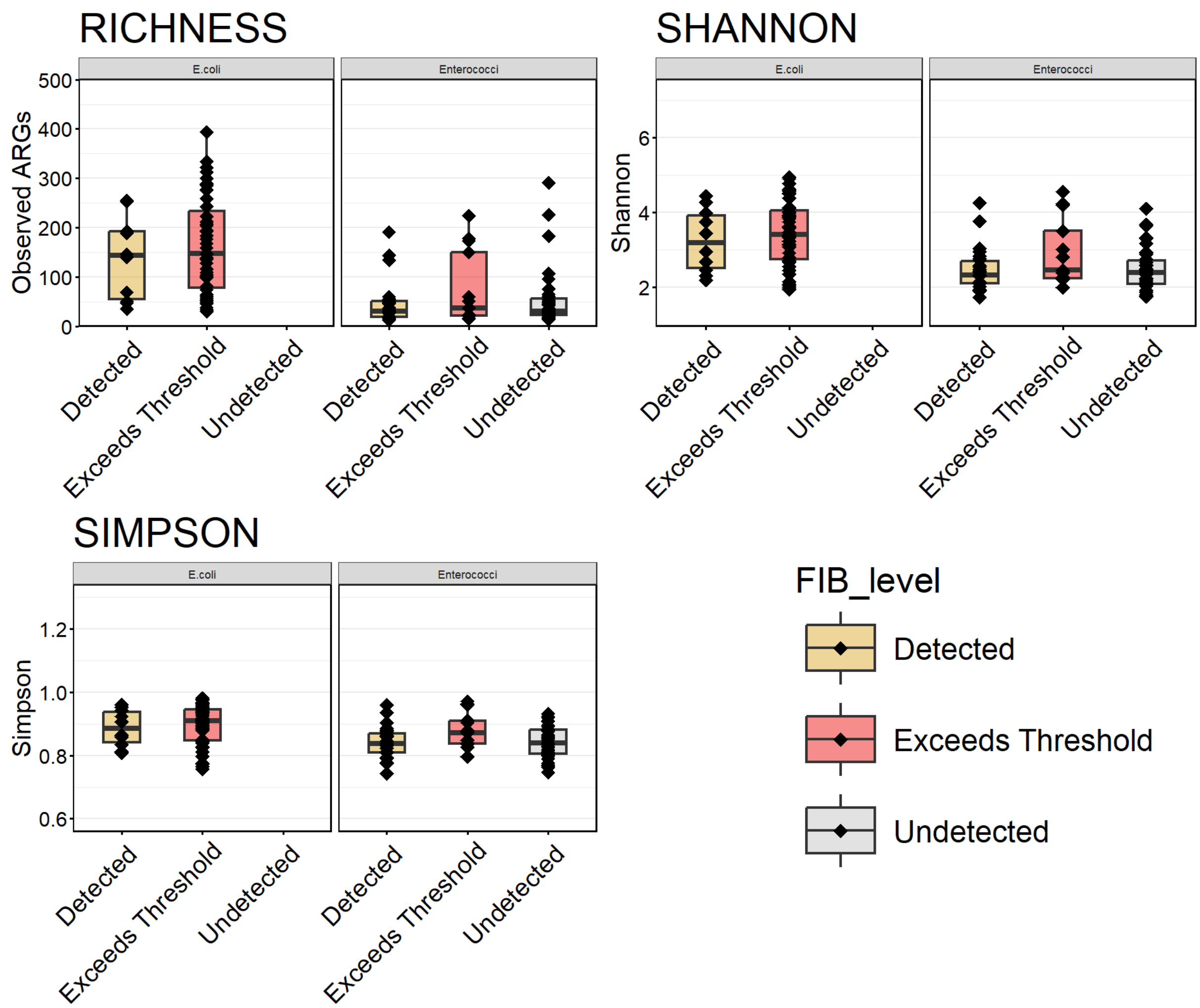

Figure 5. A boxplot of alpha diversity metrics (richness, Shannon-Weiner Index, Simpson's Diversity Index) grouped by FIB level. Samples within marine sites (Los Olmos and Baffin Bay) were tested for FIB using enterococci, while freshwater sites were tested for FIB using *E. coli*. The FIB levels were determined using FIB-associated LODs and risk thresholds.

Significant correlations between alpha diversity and other variables were identified (Table 1). There were strong positive correlations between all alpha diversity metrics and the human, pig, and cow MST fecal markers. Dissolved oxygen, water temperature, and rainfall had no significant correlations with alpha diversity, while conductivity showed a strong negative correlation with all alpha diversity metrics. Nitrate, dissolved organic nitrogen, and total phosphate had significant positive correlations with all diversity metrics, while nitrite showed a significant negative correlation with all diversity metrics. Ammonia concentrations were significantly positively correlated with Shannon's and Simpson's diversity indices, but showed no correlation with richness, whereas chlorophyll *a* was significantly positively correlated with richness but not with Shannon's or Simpson's diversity indices.

Table 1. Spearman's rank correlation coefficients between alpha diversity metrics, MST markers, environmental parameters, and nutrient concentrations. *** p<0.001, ** p<0.01, * p<0.05 and ˙ p<0.1.

	Parameter	*Observed*	*Shannon*	*Simpson*
MST Markers (gene copies/100mL)	Human	**0.3712*** **	**0.328*** **	**0.299*** **
	Gull	-0.117	-0.128	-0.129
	Pig	**0.368*** **	**0.409*** **	**0.420 *** **
	Cow	**0.436*** **	**0.435*** **	**0.421*** **
Environmental Parameters	Weighted rainfall (mm)	0.125	0.135˙	0.162˙
	Dissolved Oxygen (mg/L)	0.135	0.007	-0.054
	Conductivity (µS/cm)	**-0.627*** **	**-0.504*** **	**-0.423*** **
	Water Temperature (˚C)	0.019	0.079	0.116
Nutrients	Nitrate	**0.259** **	**0.219*** **	**0.196* **
	Nitrite	**-0.200* **	**-0.204* **	**-0.207* **
	Ammonia	0.150˙	**0.180* **	**0.186* **
	Dissolved Organic Nitrogen	**0.196* **	**0.255** **	**0.267** **
	Total Phosphate	**0.517*** **	**0.544*** **	**0.535*** **
	Chlorophyll *a*	**0.184* **	0.152˙	0.139˙
FIB Concentrations (MPN/100mL)	*E. coli*	-0.207	-0.216	-0.225˙
	Enterococci	0.024	0.113	0.140

Beta Diversity

Location was a significant source of variation within the resistome across the watershed. NMDS plots using both Jaccard's Similarity and Bray-Curtis Dissimilarity distances showed slight clustering by system, with the tightest clustering exhibited among samples originating from San

Fernando Creek (Figure 6). Minimal clustering due to seasonal grouping was observed. A PERMANOVA showed that resistome composition varies significantly by system (R^2=0.455, p=0.001) and season (R^2=0.050, p=0.002). However, the sum of squares shows that the system had a stronger influence on resistome composition, explaining 45.5% of the variation, while season accounted for 5.0%. A permutation dispersal test showed no differences due to dispersion in either system or season (p=0.67, p=0.62), indicating that the differences in resistome composition are not driven by dispersion and are true differences driven by system and season.

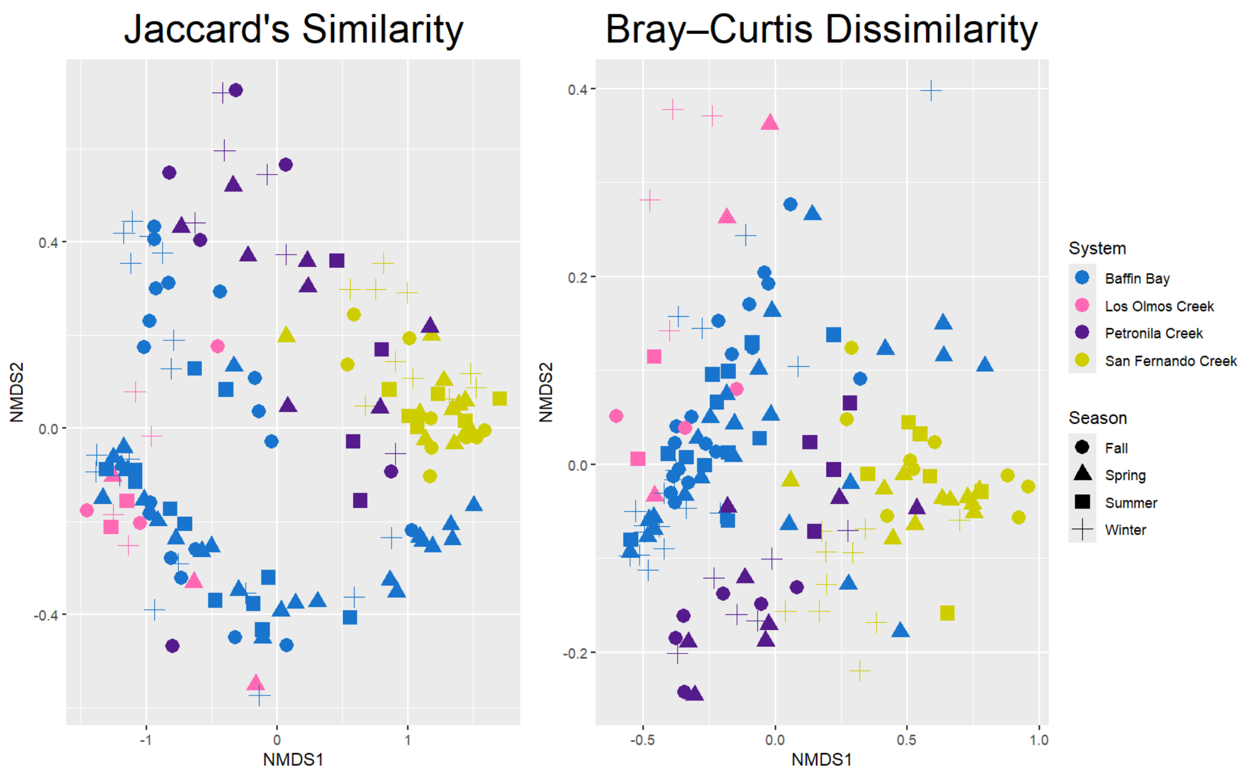

Figure 6. NMDS plots showing ARG beta diversity using Jaccard's Similarity and Bray-Curtis Dissimilarity calculated from normalized ARG abundances. Each point represents an individual sample; colors indicate system and shapes indicate season.

A relative abundance plot grouped by system showed that all systems had high mean relative abundances of aminoglycoside, erythromycin, fluoroquinolone, macrolide-lincosamide-streptogramin (MLS), rifampin, and tetracycline resistance genes (Figure 7). Additionally, San Fernando Creek had a higher mean relative abundance of drug and biocide resistance ARGs, as well as multidrug and multimetal resistance ARGs. Los Olmos Creek had the highest mean relative abundance of ARGs for *Mycobacterium tuberculosis* specific drugs than all other systems. Relative abundance and its spatial patterns are shown in Figure S1. The dendrogram indicates tight clustering of San Fernando Creek samples, while relative abundance profiles were largely uniform across Baffin Bay, Petronila Creek, and Los Olmos Creek.

Figure 7. The mean relative abundance plots of ARG classes, grouped by water system. Each bar represents the mean across all samples within a system.

Differential Abundance Between Baffin Bay and its Tributaries

Compared with Baffin Bay, the San Fernando Creek resistome had the highest overall number of ARG classes with significant differential abundances that passed sensitivity testing. San Fernando Creek had significantly higher abundances of drug and biocide, MLS, multidrug resistant, rifampin, tetracyclines, *M. tuberculosis* specific drugs, biocide and metal, mercury, copper, and several other classes of ARGs than Baffin Bay, with drug and biocide ARGs having the highest absolute fold increase. Additionally, San Fernando Creek has significantly fewer ARGs from the aminoglycoside class than Baffin Bay. Petronila Creek contained a significantly higher absolute fold increase in fluoroquinolone and mercury resistance than Baffin Bay. Petronila Creek also showed a significant absolute fold decrease in phenicol resistance than Baffin Bay. An increase in *M. tuberculosis* specific drug resistance genes within Los Olmos Creek is the only significantly different class of ARGs that passed sensitivity testing.

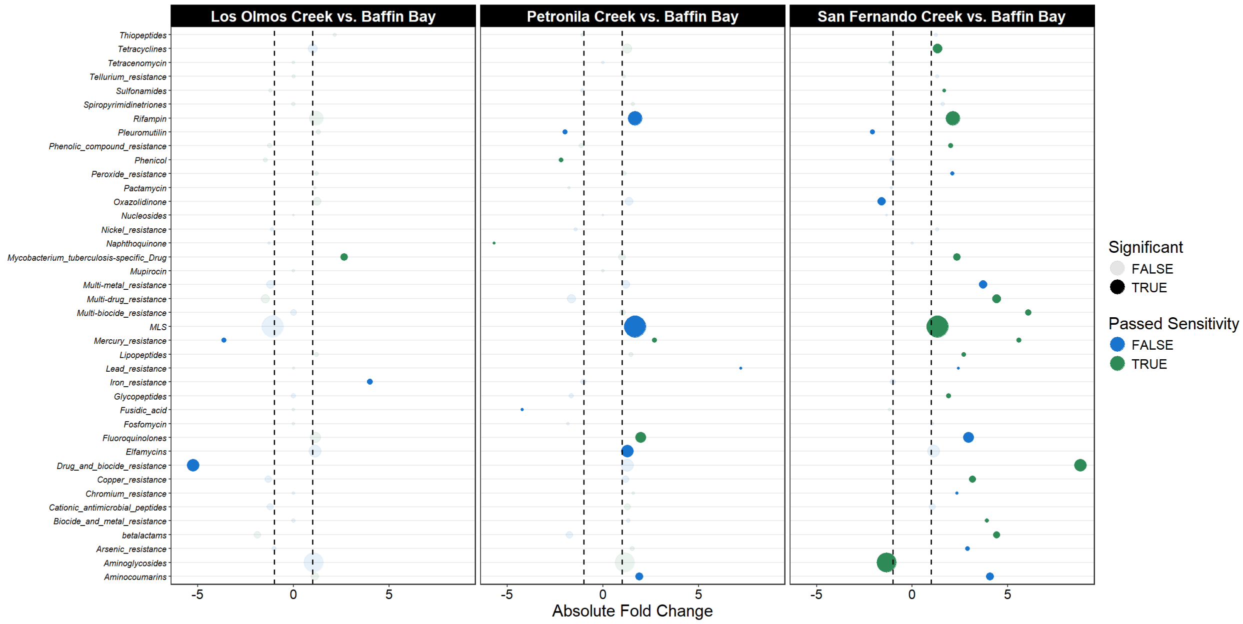

Figure 8. Differential abundance plot of the absolute fold change of ARG classes of each tributary compared to Baffin Bay. Shaded circles represent significant changes in ARG differential abundance ($p<0.05$), while transparent circles represent nonsignificant changes in ARG differential abundance.

Discussion

The resistome of the Baffin Bay watershed is primarily influenced by location, land use, fecal pollution, and to a lesser extent, seasonality. Southern Texas experiences weak seasons, and the only increase in ARG diversity occurred between winter and spring. Land use varies across the watershed, and each freshwater inflow experiences unique anthropogenic stressors that contribute to significant differences in the resistome. The most prominent example is San Fernando Creek, where ARGs were more abundant and diverse than all other systems. The land surrounding Baffin Bay, Los Olmos Creek, and Petronila Creek is mostly rural and used for agriculture and livestock ranches (Gregory et al., 2022). Conversely, San Fernando Creek runs through livestock ranches and a major population center in the city of Kingsville, TX (pop. 24,884), which is home to the only hospital within the watershed (Gregory et al., 2022). Urban populations, hospitals, and livestock contribute to enrichment of AMR through runoff, wastewater outflows, and manure (FAO, 2020).

Higher ARG abundance and richness were observed in Petronila Creek compared to Baffin Bay and Los Olmos Creek. Petronila also showed distinct differences in beta diversity including clustering in the NMDS plot and higher mercury resistance, higher fluoroquinolone resistance, and lower phenicol resistance than Baffin Bay. ARG enrichment and diversity can be driven by population growth, herbicides, and pesticides (FAO, 2020). Therefore, the resistome of Petronila Creek may be attributable to stressors such as urban sprawl originating from Corpus Christi, runoff from cultivated crops, and small towns and colonias that Petronila Creek flows through, such as Driscoll, TX (pop. 680) and Petronila, TX (pop. 89) (Gregory et al., 2022).

Los Olmos Creek and Baffin Bay exhibited similarity and uniformity in beta diversity, with only one class of ARGs (*M. tuberculosis* specific drugs) showing a significant increase in differential abundance in Los Olmos Creek. Both systems are classified as marine sites as Los Olmos Creek experiences tidal backflow, low inflow, and high evaporation (Gregory et al., 2022). Los Olmos Creek had a significantly higher abundance of ARGs than Baffin Bay, but significantly lower ARG richness. These differences may be due to land use. Los Olmos Creek is predominantly surrounded by rural livestock ranches, which may result in strong, uniform stressors, leading to high abundances of ARGs with low richness (Gregory et al., 2022). On the other hand, Baffin Bay is a larger, dynamic system that is also impacted by inflow from Petronila and San Fernando Creeks.

The highest relative abundances of ARGs in the Baffin Bay watershed were observed in the aminoglycoside and MLS resistant classes. Each system also contained ARGs within the rifampin, elfamycin, tetracycline, and fluoroquinolone resistance classes. These five classes of ARGs confer resistance to potent antibiotics used to treat bacterial infections in humans and livestock. Additionally, aminoglycoside, elfamycin, MLS, and tetracycline resistance class ARGs were present in every sample (Figure S1). The omnipresence of these ARG classes suggests that watershed-wide ARG sources or selection pressures play a role in shaping the resistome.

Cattle ranching, which is common throughout the watershed, may be driving the watershed-wide patterns in the resistome. Aminoglycosides, tetracyclines, and MLS antibiotics are among the most widely sold for livestock in the United States. Tetracyclines account for 37% of annual sales by mass, followed by macrolides (5%) and aminoglycosides (3%). (2023 Summary Report On Antimicrobials Sold or Distributed for Use in Food-Producing Animals, 2024). All three are sold predominantly for cattle compared to other livestock species. Currently, elfamycins are an understudied class of antibiotics that show potential as growth promoters and may be used throughout the lifespan of livestock (Landers et al., 2012; Maiese et al., 1989; Mathew et al., 2007; Sarmah et al., 2006). Livestock production and manure runoff from the extensive ranches in the watershed may contribute to the consistent, high relative abundances of aminoglycosides, macrolides, tetracycline, and potentially elfamycin ARGs.

Surprisingly, low relative abundances of metal resistance were observed within all systems. Previous studies have detected heavy metals in Baffin Bay and the neighboring Upper Laguna Madre (Douglas et al., 2025; Sharma et al., 1999). However, metal resistance within the watershed was primarily observed in the freshwater tributaries. Both San Fernando Creek and Petronila Creek had higher differential abundances of heavy metal ARGs than Baffin Bay. Petronila Creek contained higher mercury resistance while San Fernando contained higher mercury, copper, and biocide and metal resistance class ARGs.

ARGs play a unique role in the environment as they are both driven and co-selected by pollutants and are pollutants themselves. Previous studies have established fecal pollution as a primary driver of ARG pollution, as humans and animals excrete residual antibiotics (FAO, 2020; Karkman et al., 2019; Larsson & Flach, 2022). The current national standard for monitoring fecal pollution within aquatic environments is FIB; acceptable concentrations of FIB (MPN/100mL) are based on a risk-based threshold of 32 illnesses/1000 recreational events (United States Environmental Protection Agency, 2011). While there are currently no requirements for monitoring ARGs within aquatic environments, reducing fecal pollution remains one of the primary strategies for mitigating ARGs in marine and freshwater environments (FAO, 2020).

Baffin Bay comprises both freshwater and marine systems, allowing exploration of the relationship between ARGs and FIBs using enterococci and *E. coli* metrics. However, no differences in ARG diversity were observed at the differing FIB levels, nor was there a correlation between FIB concentrations and ARG diversity. FIB has received criticism for false positives in both marine and freshwater environments and its inability to distinguish different sources of fecal pollution; both *E.coli* and enterococci to have been found to establish themselves as resident bacteria in the water column, sand, and benthic environments and inflate FIB concentrations (Graves et al., 2023; Ishii et al., 2007; Ishii & Sadowsky, 2008; Mika et al., 2014; Mote et al., 2012; N. C. Powers et al., 2025). In this study, resistome alpha diversity was positively correlated with human, pig, and cow fecal pollution. Since fecal pollution is tightly linked with ARGs, the lack of association between ARGs and FIB in both marine and freshwater environments suggests that FIB is not an adequate proxy for ARG pollution in this system.

As ARGs become recognized as pollutants in estuarine and marine environments, understanding their drivers and characterizing the resistome composition will become crucial for monitoring and mitigation. These results advance our understanding of resistome dynamics in hypersaline systems. Within Baffin Bay, the resistome is less affected by seasonal variation and more strongly influenced by land-use activities such as ranching, agriculture, and upstream urbanization. Bacterial antibiotics used in the cattle industry likely select for the abundance and persistence of the dominant ARGs. Anthropogenic pollution mitigation within Baffin Bay has been hindered by the limitations of FIB. This data suggests that FIB is not an adequate indicator of AMR within Baffin Bay and its tributaries. Determining an adequate proxy for ARG monitoring and mitigating source-specific fecal pollution will play a critical role in the future of AMR management within the TCB.

Conclusions

- ARGs were detected in all water samples. San Fernando Creek contained the highest abundance of positive hits for ARGs.
- Alpha diversity and beta diversity were primarily influenced by location. San Fernando Creek posted significantly higher richness, Shannon-Wiener, and Simpson's Diversity than Baffin Bay, Petronila Creek, and Los Olmos Creek.
- Seasonality accounted for a small percentage of variation in the resistome. Changes in the resistome diversity due to season occurred only between winter and spring.
- Alpha diversity was positively correlated with fecal pollution originating from humans, pigs, and cows. Alpha diversity was also positively correlated with nutrient pollution, including nitrate, ammonia, dissolved organic nitrogen, total phosphate, and chlorophyll *a*. These correlations suggest that fecal and nutrient pollution are drivers and predictors of ARG pollution within the watershed. Lastly, alpha diversity showed a strong negative correlation with conductivity, likely due to the distinct differences in salinities within each system.
- ARGs for bacterial antibiotics such as aminoglycosides, MLS, elfamycins, fluoroquinolones, tetracyclines, and rifampins had high mean relative abundances in all water systems. Additionally, aminoglycoside, MLS, elfamycin, and tetracycline class ARGs were present in all samples.
- Drug and biocide resistance, multidrug resistance, and multibiocide resistance had higher relative abundances and significantly higher differential abundance in San Fernando Creek.
- Los Olmos Creek contained ARGs for *M. tuberculosis* specific drugs in a higher mean relative abundance and a significantly higher differential abundance than all other systems.
- Neither FIB (enterococci in marine systems and *E. coli* in freshwater systems) was a driver of AMR. Whether or not FIB was undetected, detected, or exceeded the risk-based threshold did not cause significant differences in alpha diversity.

References

2023 Summary report on antimicrobials sold or distributed for use in food-producing animals. (2024). U.S. Food and Drug Administration. https://www.fda.gov/animal-veterinary/antimicrobial-resistance/2023-summary-report-antimicrobials-sold-or-distributed-use-food-producing-animals

Agramont, J., Gutiérrez-Cortez, S., Joffré, E., Sjöling, Å., & Calderon Toledo, C. (2020). Fecal pollution drives antibiotic resistance and class 1 Integron abundance in aquatic environments of the Bolivian Andes impacted by mining and wastewater. *Microorganisms*, *8*(8), 1122. https://doi.org/10.3390/microorganisms8081122

Ahlmann-Eltze, C., & Patil, I. (2021). *ggsignif: R package for displaying significance brackets for "ggplot2."* https://doi.org/10.31234/osf.io/7awm6

Ahmed, S. A., Barış, E., Go, D. S., Lofgren, H., Osorio-Rodarte, I., & Thierfelder, K. (2018). Assessing the global poverty effects of antimicrobial resistance. *World Development*, *111*, 148–160. https://doi.org/10.1016/j.worlddev.2018.06.022

Almeida, A., Loy, A., & Hofmann, H. (2019). Ggplot2 compatible quantile-quantile Plots in R. *The R Journal*, *10*(2), 248. https://doi.org/10.32614/RJ-2018-051

Andrews, S. (2010). *FastQC: A quality control tool for high throughput sequence data [Online]. Available online* [Computer software].

Bokulich, N. A., Subramanian, S., Faith, J. J., Gevers, D., Gordon, J. I., Knight, R., Mills, D. A., & Caporaso, J. G. (2013). Quality-filtering vastly improves diversity estimates from Illumina amplicon sequencing. *Nature Methods*, *10*(1), 57–59. https://doi.org/10.1038/nmeth.2276

Bolger, A. M., Lohse, M., & Usadel, B. (2014). Trimmomatic: A flexible trimmer for Illumina sequence data. *Bioinformatics*, *30*(15), 2114–2120. https://doi.org/10.1093/bioinformatics/btu170

Bonin, N., Doster, E., Worley, H., Pinnell, L. J., Bravo, J. E., Ferm, P., Marini, S., Prosperi, M., Noyes, N., Morley, P. S., & Boucher, C. (2023). MEGARes and AMR++, v3.0: An updated comprehensive database of antimicrobial resistance determinants and an improved software pipeline for classification using high-throughput sequencing. *Nucleic Acids Research*, *51*(D1), D744–D752. https://doi.org/10.1093/nar/gkac1047

CDC. (2019). *Antibiotic resistance threats in the United States*. U.S Department of Health and Human Services.

Conkle, J., & Hormoz-Estrabad, Z. (2018). *Pesticide loading and sediment accumulation in Baffin Bay: addressing an important stakeholder concern regarding the bay's health* (16-062-

000–9106). https://www.glo.texas.gov/sites/default/files/2025-10/pesticide-loading-and-final-report.pdf

D'Costa, V. M., King, C. E., Kalan, L., Morar, M., Sung, W. W. L., Schwarz, C., Froese, D., Zazula, G., Calmels, F., Debruyne, R., Golding, G. B., Poinar, H. N., & Wright, G. D. (2011). Antibiotic resistance is ancient. *Nature*, *477*(7365), 457–461. https://doi.org/10.1038/nature10388

Douglas, A. R., Montagna, P. A., & Dellapenna, T. (2025). Influence of inflows on estuary sediments. In P. A. Montagna & A. R. Douglas (Eds.), *Freshwater Inflows to Texas Bays and Estuaries* (pp. 173–190). Springer Nature Switzerland. https://doi.org/10.1007/978-3-031-70882-4_6

FAO. (2020). *Technical brief on water, sanitation, hygiene and wastewater management to prevent infections and reduce the spread of antimicrobial resistance*. http://www.fao.org/3/ca9120en/CA9120EN.pdf

Graves, G. M., Tanner, R. S., Vogel, J. R., De León, K. B., & Walls, A. W. (2023). The effect of Paenibacillus on IDEXX Enterolert results from freshwater stream environments. *Environmental Science and Pollution Research*, *30*(39), 91074–91083. https://doi.org/10.1007/s11356-023-28797-y

Gregory, L., Escamilla, C., & Rios, E. (2022, June). *San Fernando and Petronila Creeks Watershed Protection Plan*. Texas Water Resources Institute. https://baffin.twri.tamu.edu/wp-content/uploads/sites/11/2023/09/San-Fernando-and-Petronila-Creeks-WPP.2023-update_opt.pdf

Hatosy, S. M., & Martiny, A. C. (2015). The ocean as a global reservoir of antibiotic resistance genes. *Applied and Environmental Microbiology*, *81*(21), 7593–7599. https://doi.org/10.1128/AEM.00736-15

Ishii, S., Hansen, D. L., Hicks, R. E., & Sadowsky, M. J. (2007). Beach sand and sediments are temporal sinks and sources of *Escherichia coli* in Lake Superior. *Environmental Science & Technology*, *41*(7), 2203–2209. https://doi.org/10.1021/es0623156

Ishii, S., & Sadowsky, M. J. (2008). Escherichia coli in the environment: implications for water quality and human health. *Microbes and Environments*, *23*(2), 101–108. https://doi.org/10.1264/jsme2.23.101

Karkman, A., Pärnänen, K., & Larsson, D. G. J. (2019). Fecal pollution can explain antibiotic resistance gene abundances in anthropogenically impacted environments. *Nature Communications*, *10*(1), 80. https://doi.org/10.1038/s41467-018-07992-3

Kim, D.-W., & Cha, C.-J. (2021). Antibiotic resistome from the One-Health perspective: Understanding and controlling antimicrobial resistance transmission. *Experimental & Molecular Medicine*, *53*(3), 301–309. https://doi.org/10.1038/s12276-021-00569-z

Landers, T. F., Cohen, B., Wittum, T. E., & Larson, E. L. (2012). A review of antibiotic use in food animals: Perspective, policy, and potential. *Public Health Reports®*, *127*(1), 4–22. https://doi.org/10.1177/003335491212700103

Larsson, D. G. J., & Flach, C.-F. (2022). Antibiotic resistance in the environment. *Nature Reviews Microbiology*, *20*(5), 257–269. https://doi.org/10.1038/s41579-021-00649-x

Lin, H., & Peddada, S. D. (2020). Analysis of compositions of microbiomes with bias correction. *Nature Communications*, *11*(1), 3514. https://doi.org/10.1038/s41467-020-17041-7

Maiese, W. M., Lechevalier, M. P., Lechevalier, H. A., Korshalla, J., Goodman, J., Wildey, M. J., Kuck, N., Conner, S. D., & Greenstein, M. (1989). LL-E19020.ALPHA. and .BETA., animal growth promoting antibiotics: Taxonomy, fermentation and biological activity. *The Journal of Antibiotics*, *42*(10), 1489–1493. https://doi.org/10.7164/antibiotics.42.1489

Mathew, A. G., Cissell, R., & Liamthong, S. (2007). Antibiotic resistance in bacteria associated with food animals: A United States perspective of livestock production. *Foodborne Pathogens and Disease*, *4*(2), 115–133. https://doi.org/10.1089/fpd.2006.0066

McMurdie, P. J., & Holmes, S. (2013). phyloseq: An R package for reproducible interactive analysis and graphics of microbiome census data. *PLoS ONE*, *8*(4), e61217. https://doi.org/10.1371/journal.pone.0061217

Mika, K. B., Ginsburg, D. W., Lee, C. M., Thulsiraj, V., & Jay, J. A. (2014). Fecal indicator bacteria levels do not correspond with incidence of human-associated HF183 bacteroides 16S rRNA genetic marker in two urban southern California watersheds. *Water, Air, & Soil Pollution*, *225*(6), 1960. https://doi.org/10.1007/s11270-014-1960-7

Mote, B. L., Turner, J. W., & Lipp, E. K. (2012). Persistence and growth of the fecal indicator bacteria enterococci in detritus and natural estuarine plankton communities. *Applied and Environmental Microbiology*, *78*(8), 2569–2577. https://doi.org/10.1128/AEM.06902-11

Naghavi, M., Vollset, S. E., Ikuta, K. S., Swetschinski, L. R., Gray, A. P., Wool, E. E., Robles Aguilar, G., Mestrovic, T., Smith, G., Han, C., Hsu, R. L., Chalek, J., Araki, D. T., Chung, E., Raggi, C., Gershberg Hayoon, A., Davis Weaver, N., Lindstedt, P. A., Smith, A. E., … Murray, C. J. L. (2024). Global burden of bacterial antimicrobial resistance 1990–2021: A systematic analysis with forecasts to 2050. *The Lancet*, *404*(10459), 1199–1226. https://doi.org/10.1016/S0140-6736(24)01867-1

Oksanen, J., Simpson, G. L., Blanchet, F. G., Kindt, R., Legendre, P., Minchin, P. R., O'Hara, R. B., Solymos, P., Stevens, M. H. H., Szoecs, E., Wagner, H., Barbour, M., Bedward, M., Bolker, B., Borcard, D., Borman, T., Carvalho, G., Chirico, M., De Caceres, M., … Weedon, J. (2001). *vegan: Community ecology package* (p. 2.7-2) [Dataset]. https://doi.org/10.32614/CRAN.package.vegan

Pinnell, L. J., Kuiper, G., Huebner, K. L., Doster, E., Parker, J. K., Alekozai, N., Powers, J. G., Wallen, R. L., Belk, K. E., & Morley, P. S. (2023). More than an anthropogenic phenomenon: Antimicrobial resistance in ungulates from natural and agricultural environments. *Science of The Total Environment*, *858*, 159789. https://doi.org/10.1016/j.scitotenv.2022.159789

Powers, N., Bleth, N., Gitter, A., Gregory, L., Wetz, M., & Turner, J. (2025). *Improving community health: Microbial source tracking and quantitative microbial risk assessment on the Texas coast* (EPA Final Report. MX-02D18222).

Powers, N. C., Gitter, A., Bleth, N., Johnson, A., Nicolay, J., Ayers, R., & Turner, J. W. (2025). Microbial source tracking in a coastal residential canal system. *Science of The Total Environment*, *983*, 179676. https://doi.org/10.1016/j.scitotenv.2025.179676

QIAGEN. (2023, June). *DNeasy® PowerSoil® pro kit handbook*. QIAGEN. https://www.qiagen.com/us/resources/resourcedetail?id=9bb59b74-e493-4aeb-b6c1-f660852e8d97&lang=en

Sarmah, A. K., Meyer, M. T., & Boxall, A. B. A. (2006). A global perspective on the use, sales, exposure pathways, occurrence, fate and effects of veterinary antibiotics (VAs) in the environment. *Chemosphere*, *65*(5), 725–759. https://doi.org/10.1016/j.chemosphere.2006.03.026

Sharma, V. K., Rhudy, K. B., Koening, R., & Vazquez, F. G. (1999). Metals in sediments of the Upper Laguna Madre. *Marine Pollution Bulletin*, *38*(12), 1221–1226. https://doi.org/10.1016/S0025-326X(99)00166-6

Su, Z., Chen, L., & Wen, D. (2024). Impact of wastewater treatment plant effluent discharge on the antibiotic resistome in downstream aquatic environments: A mini review. *Frontiers of Environmental Science & Engineering*, *18*(3), 36. https://doi.org/10.1007/s11783-024-1796-3

Texas General Land Office. (n.d.). *Texas Beach Watch*. Retrieved November 6, 2024, from https://www.texasbeachwatch.com/

United States Environmental Protection Agency. (2011). *Ambient water criteria for bacteria.*

Wilke, C. O. (2015). *cowplot: Streamlined plot theme and plot annotations for "ggplot2"* (p. 1.2.0) [Dataset]. https://doi.org/10.32614/CRAN.package.cowplot

Withers, K., Chapman, B., Tunnell, J., & Judd, F. (2002). *The Laguna Madre of Texas and Tamaulipas* (1–2). Texas A&M University Press.

Wright, G. D. (2007). The antibiotic resistome: The nexus of chemical and genetic diversity. *Nature Reviews Microbiology*, *5*(3), 175–186. https://doi.org/10.1038/nrmicro1614

Xu, N., Qiu, D., Zhang, Z., Wang, Y., Chen, B., Zhang, Q., Wang, T., Hong, W., Zhou, N.-Y., Penuelas, J., Gillings, M., Zhu, Y.-G., & Qian, H. (2023). A global atlas of marine antibiotic resistance genes and their expression. *Water Research*, *244*, 120488. https://doi.org/10.1016/j.watres.2023.120488

Zheng, D., Yin, G., Liu, M., Chen, C., Jiang, Y., Hou, L., & Zheng, Y. (2021). A systematic review of antibiotics and antibiotic resistance genes in estuarine and coastal environments. *Science of The Total Environment*, *777*, 146009. https://doi.org/10.1016/j.scitotenv.2021.146009

Zhu, Y.-G., Zhao, Y., Li, B., Huang, C.-L., Zhang, S.-Y., Yu, S., Chen, Y.-S., Zhang, T., Gillings, M. R., & Su, J.-Q. (2017). Continental-scale pollution of estuaries with antibiotic resistance genes. *Nature Microbiology*, *2*(4), 16270. https://doi.org/10.1038/nmicrobiol.2016.270

Supplemental

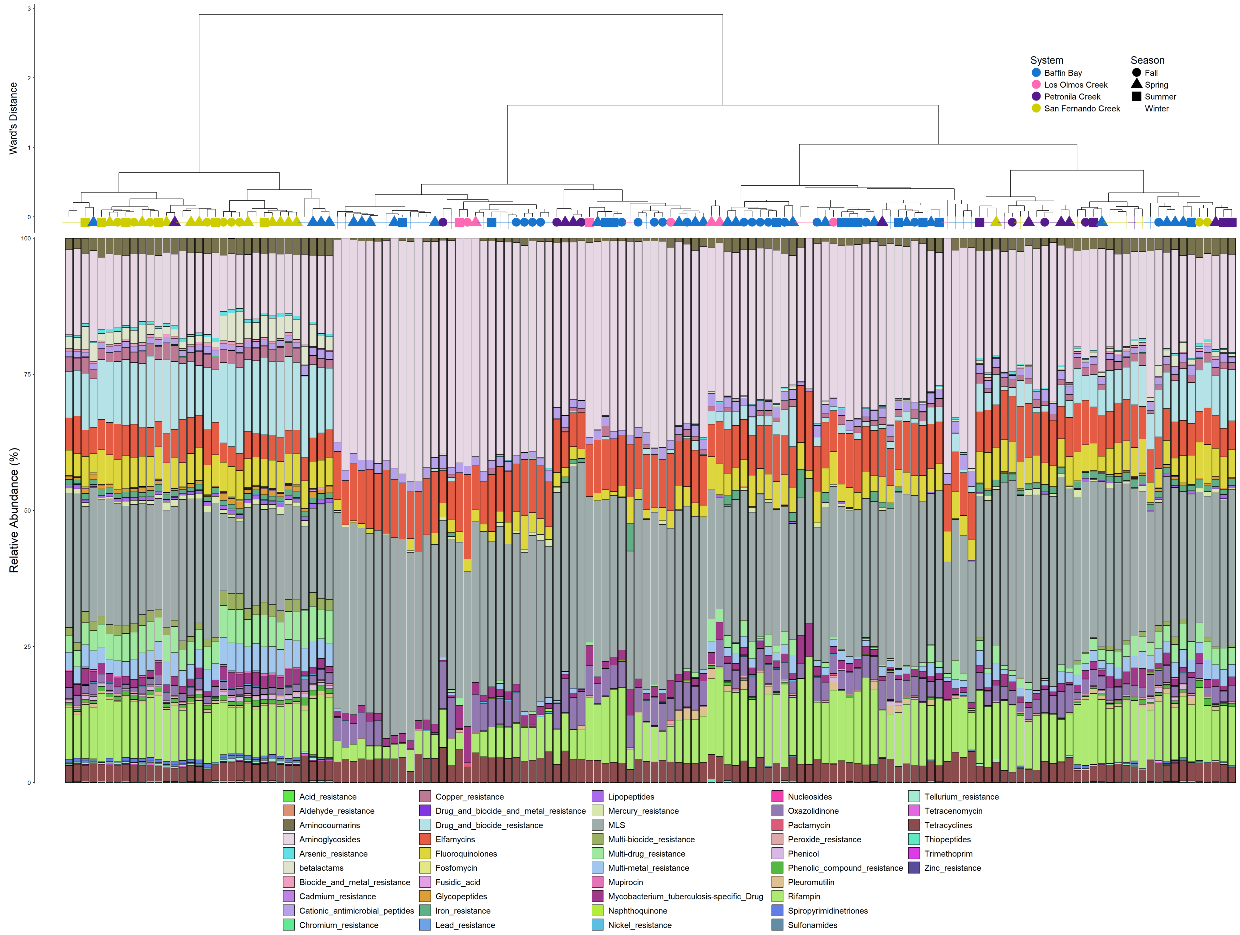

Figure S1. A relative abundance plot of all samples within the study (N=144) paired with a dendrogram using Bray-Curtis's distance matrix. Each bar represents one sample within the study; the shape within the dendrogram represents season, and color represents each sample's corresponding water system.

Table S1. List of samples processed for resistome analysis, describing the DNA concentration (ng/L) and quality (A260, A260/280, A260/230).

Sampling Date	Site	Concentration ng/L	A260	A260/280	A260/230	Sample ID
6/8/2023	13033	94.5	0.379	1.68	1.04	1
6/8/2023	13034	236.4	0.532	1.79	1.01	2
6/8/2023	13094	74.2	0.231	1.74	0.42	3
6/8/2023	13096	51.8	0.156	1.72	0.8	4
6/8/2023	15969	102.8	0.263	1.75	1.45	5

6/8/2023	22327	66.4	0.209	1.69	0.69	6
9/5/2023	13033	49.3	0.218	1.72	0.64	7
9/5/2023	13034	69.7	0.254	1.73	1.37	8
9/5/2023	13094	48.1	0.19	1.79	0.63	9
9/5/2023	13096	56	0.235	1.77	0.5	10
9/5/2023	15969	100.5	0.408	1.7	1.33	11
9/5/2023	22327	64.1	0.223	1.83	0.95	12
10/4/2023	13033	76.6	0.279	1.79	1.25	13
10/4/2023	13034	121.6	0.293	1.82	1.26	14
10/4/2023	13094	44.4	0.166	1.73	0.92	15
10/4/2023	13096	14.2	0.135	1.76	0.78	16
10/4/2023	15969	110.9	0.14	1.86	1.54	17
10/4/2023	22327	39.8	0.189	1.7	0.81	18
11/8/2023	13033	53.2	0.04	1.82	1.31	19
11/8/2023	13034	167.4	0.313	1.83	1.45	20
11/8/2023	13094	26.4	0.19	1.64	0.95	21
11/8/2023	13096	20.8	0.191	1.76	0.59	22
11/8/2023	15969	118.8	0.397	1.77	0.83	23
11/8/2023	22327	38.6	0.16	1.8	1.43	24
12/5/2023	13033	39.4	0.039	1.85	1.02	25
12/5/2023	13034	303.6	0.71	1.8	1.17	26
12/5/2023	13094	30.9	0.163	1.68	0.1	27
12/5/2023	13096	43.3	0.248	1.68	0.82	28
12/5/2023	15969	64.4	0.292	1.73	0.64	29
12/5/2023	22327	19.6	0.079	1.79	0.56	30
1/11/2024	13033	51.9	0.234	1.8	0.34	31
1/11/2024	13034	108.5	0.333	1.79	0.68	32
1/11/2024	13094	29.7	0.086	1.84	0.72	33
1/11/2024	13096	49.1	0.216	1.68	0.58	34
1/11/2024	15969	45.5	0.206	1.7	0.88	35
2/9/2023	22327	29	0.133	1.58	0.73	36
2/6/2024	13033	38.7	0.265	1.68	0.43	37
2/6/2024	13034	416.9	1.047	1.78	1.17	38
2/6/2024	13094	46.8	0.286	1.67	0.89	39
2/6/2024	13096	64.1	0.306	1.76	0.75	40
2/6/2024	15969	66.1	0.332	1.69	0.49	41
2/6/2024	22327	29	0.168	1.75	0.27	42
4/6/2023	13033	71.6	0.238	1.8	1.09	43
4/6/2023	13034	211.8	0.51	1.83	1.55	44
4/6/2023	13094	61.4	0.166	1.83	1.09	45
4/6/2023	13096	70.6	0.166	1.78	1.58	46

4/6/2023	15969	66	0.257	1.76	1.16	47
4/6/2023	22327	57.8	0.19	1.76	0.89	48
2/9/2023	13033	47.9	0.164	1.66	0.74	49
3/13/2024	13034	273.2	0.671	1.81	1.39	50
3/13/2024	13094	96.3	0.395	1.71	1.26	51
3/13/2024	13096	58.8	0.276	1.72	0.31	52
3/13/2024	15969	85.8	0.027	1.89	0.57	53
3/13/2024	22327	42.7	0.25	1.65	0.65	54
3/9/2023	13033	82.2	0.313	1.64	0.78	55
2/9/2023	13034	64.9	0.265	1.63	0.65	56
4/11/2024	13094	86.5	0.354	1.75	0.61	57
4/11/2024	13096	52.5	0.226	1.74	0.49	58
4/11/2024	15969	91.4	0.392	1.75	0.73	59
4/11/2024	22327	63.7	0.177	1.82	0.86	60
5/22/2024	13033	35.7	0.323	1.66	0.31	61
5/22/2024	13034	424	1.023	1.79	0.95	62
5/22/2024	13094	80.2	0.352	1.72	1.08	63
5/22/2024	13096	75.9	0.286	1.77	1.38	64
5/22/2024	15969	66.4	0.177	1.84	0.79	65
5/22/2024	22327	29.7	0.148	1.85	0.14	66
6/12/2024	13033	53.2	0.091	1.83	0.74	67
6/12/2024	13034	404.8	0.795	1.8	1.53	68
6/12/2024	13094	48.2	0.245	1.64	0.6	69
6/12/2024	13096	113.1	0.294	1.8	0.12	70
6/12/2024	15969	86	0.081	1.9	0.18	71
6/12/2024	22327	46.5	0.014	1.98	0.83	72
4/4/2023	BB1	156.2	0.0464	1.75	1.87	73
4/4/2023	BB2	230.2	0.673	1.74	1.43	74
4/4/2023	BB3	194.2	0.625	1.76	1.5	75
4/4/2023	BB4	201.1	0.646	1.74	1.72	76
4/4/2023	BB5	147.9	0.552	1.72	1.59	77
4/4/2023	BB6	167.1	0.366	1.81	1.88	78
6/6/2023	BB1	76.2	0.333	1.7	1.41	79
6/6/2023	BB2	58.5	0.295	1.65	0.74	80
6/6/2023	BB3	45.3	0.23	1.69	0.48	81
6/6/2023	BB4	42.6	0.172	1.73	0.6	82
6/6/2023	BB5	35.8	0.097	1.7	0.54	83
6/6/2023	BB6	32.9	0.108	1.69	0.9	84
9/7/2023	BB1	79.9	0.332	1.69	0.73	85
9/7/2023	BB2	97.5	0.762	1.65	1.39	86
9/7/2023	BB3	106.2	0.277	1.8	1.43	87

9/7/2023	BB4	81.6	0.233	1.8	1.38	88
9/7/2023	BB5	92.4	0.268	1.77	1.5	89
9/7/2023	BB6	128.1	0.463	1.74	1.42	90
10/3/2023	BB1	119.8	0.458	1.71	0.53	91
10/3/2023	BB2	57.7	0.102	1.85	0.34	92
10/3/2023	BB3	86.2	0.288	1.75	1.09	93
10/3/2023	BB4	72.5	0.188	1.82	0.35	94
10/3/2023	BB5	93.4	0.296	1.77	0.48	95
10/3/2023	BB6	85.8	0.291	1.74	0.96	96
11/7/2023	BB1	107	0.364	1.77	0.5	97
11/7/2023	BB2	95.9	0.236	1.78	0.86	98
11/7/2023	BB3	124.3	0.307	1.8	0.92	99
11/7/2023	BB4	106.1	0.331	1.76	1.2	100
11/7/2023	BB5	116.5	0.413	1.74	0.85	101
11/7/2023	BB6	93.6	0.348	1.75	1.01	102
12/5/2023	BB1	92.4	0.272	1.8	1.4	103
12/5/2023	BB2	87.9	0.526	1.62	0.43	104
12/5/2023	BB3	83	0.279	1.77	0.66	105
12/5/2023	BB4	74.4	0.288	1.75	1.04	106
12/5/2023	BB5	74.3	0.3	1.73	0.57	107
12/5/2023	BB6	62.1	0.281	1.74	0.8	108
1/11/2024	BB1	148.1	0.418	1.79	1.63	109
1/11/2024	BB2	152	0.355	1.81	0.77	110
1/11/2024	BB3	141.5	0.406	1.78	1.67	111
1/11/2024	BB4	137.9	0.607	1.68	0.73	112
1/11/2024	BB5	133.6	0.43	1.75	0.51	113
1/11/2024	BB6	113.2	0.42	1.72	1.26	114
2/6/2024	BB1	114.2	0.402	1.72	0.94	115
2/6/2024	BB2	161.7	0.545	1.73	1.66	116
2/6/2024	BB3	135.2	0.369	1.79	1.34	117
2/6/2024	BB4	119.5	0.285	1.79	1.5	118
2/6/2024	BB5	122.4	0.353	1.76	1.45	119
2/6/2024	BB6	99.1	0.32	1.75	1.55	120
3/13/2024	BB1	219.7	0.514	1.8	1.81	121
3/13/2024	BB2	181.5	0.414	1.81	1.83	122
3/13/2024	BB3	163.8	0.453	1.75	1.84	123
3/13/2024	BB4	153.8	0.387	1.78	0.88	124
3/13/2024	BB5	138.7	0.36	1.78	1.52	125
3/13/2024	BB6	112.9	0.307	1.79	1.19	126
4/11/2024	BB1	235.5	0.503	1.79	1.21	127
4/11/2024	BB2	187.6	0.303	1.85	0.49	128

4/11/2024	BB3	155.3	0.235	1.84	0.81	129
4/11/2024	BB4	175.9	0.426	1.77	0.89	130
4/11/2024	BB5	157.9	0.247	1.83	0.74	131
4/11/2024	BB6	164.4	0.288	1.81	1.11	132
5/22/2024	BB1	182.7	0.147	1.84	1	133
5/22/2024	BB2	205	0.273	1.84	0.46	134
5/22/2024	BB3	154.4	0.225	1.84	0.92	135
5/22/2024	BB4	145	0.204	1.84	1.58	136
5/22/2024	BB5	140.5	0.198	1.83	1.42	137
5/22/2024	BB6	133.1	0.397	1.76	0.91	138
6/12/2024	BB1	155.5	0.545	1.75	1.41	139
6/12/2024	BB2	94.3	0.268	1.83	0.18	140
6/12/2024	BB3	199.2	0.631	1.77	1.55	141
6/12/2024	BB4	126.5	0.448	1.75	1.22	142
6/12/2024	BB5	110.5	0.39	1.74	0.67	143
6/12/2024	BB6	112.4	0.369	1.76	0.67	144